A method for evaluating both shading and power generation effects of rooftop solar PV panels for different climate zones of China

Dengjia Wang[a*], Ting Qi[a], Yanfeng Liu[a], Yingying Wang[a], Jianhua Fan[b], Yue Wang[a], Hu Du[c]

a: State Key Laboratory of Green Building in Western China, Xi'an University of Architecture and Technology, Xi'an, Shaanxi 710055, China

b: Department of Civil Engineering, Technical University of Denmark, Brovej 118, Kgs.Lyngby DK2800, Denmark

c: Welsh School of Architecture, Cardiff University, Cardiff CF103NB, UK

Highlights

- A model for evaluating both shading and power generation effects of PV roof was proposed.
- The comprehensive energy saving effects of shading and power generation was investigated.
- The application of PV roofs in 13 respective cities of China was studied and analyzed.

Abstract

The photovoltaic (PV) roofs have two main energy-saving effects, which are shading and power supply. Considering the shading and power generation gain jointly, a roof is changed from the building energy end to the building energy supply end, thus changing its energy use system greatly. Therefore, this paper carries out research on the comprehensive energy-saving effect integrating the shading and the power supply gain. Three types of PV rooftops, namely, horizontally-mounted overhead PV rooftop, tilted overhead PV rooftop, and attached PV rooftop are studied to explore their impacts on the heat gain and heat loss of the roof and building's heating and cooling load. In order to estimate the overall energy-saving in different climatic regions in China, an overall energy-saving evaluation method that considers the power generation and shading benefit effects of the PV rooftop is proposed. Based on the climate and solar radiation zones in China, 13 respective cities are selected to be included in the research. The results show that, by considering only the shading effect of PV panels, the tilted PV is more suitable in summer, reducing the heat input, whereas the horizontally-mounted PV is more effective in winter to prevent more heat loss. Regarding the overall energy-saving that considers both the shading and power generation effects of PV panels, building with horizontally-mounted PV rooftop has the highest efficiency in the summer season, while the building with tilted PV rooftop has the highest efficiency in the winter season. The model and analysis of the overall energy-saving presented in this work can provide a guide for the application of rooftop solar PV panels in different climate zones in China.

Keywords

Rooftop PV, Shading benefit, Power generation, Overall energy-saving efficiency

1. Introduction

Due to the conventional energy shortage and environmental deterioration, the development and utilization of renewable energy have become inevitable in order to overcome the current energy crisis. Among various of renewable energy sources, solar energy has gathered significant attention due to its abundance, universality, and cleanliness. Further, among all the emerging solar technologies, the photovoltaic (PV) is one of the most affordable promising approaches that can meet future energy needs and alleviate environmental problems (Jung, 2014). However, the performance of PV systems is affected by different factors. For instance, the electricity generation performance of PV system is unstable due to intermittent sunlight, temperature difference, latitude, module configuration, shading, and other factors. Therefore, in order to achieve the efficient and stable operation of a PV system, the PV system needs to be optimized.

Topić et al. (2017) established a mathematical model to find the optimal PV configuration and inclination angle for a given installation area. Their model considered the influence of inter-row shading on the output power of PV module, introduced shading factor, and given the optimal row number and module angle according to the ratio of the sunlight part of the PV module to the whole module surface. Bai et al. (2015) put forward a method to simulate the output characteristics of a PV system under partial shading or mismatch conditions. In order to evaluate the effectiveness of this method, the I-V and P-V curves of a PV system under the predetermined local occlusion and mismatching conditions were compared experimentally. The experimental results showed that this method could accurately simulate the I-V and P-V characteristics of PV modules or arrays. Renaudineau et al. (2011) proposed a maximum power point tracking algorithm (MPPT) based on load characteristics. In addition, the proposed MPPT solved the shadow problem, so the power load characteristics could present two or more local maximums that were close to each other. Ghoddami and Yazdani (2011) developed a single-stage and three-phase PV power generation system with the strengthened ability to track the maximum power point and improved energy output under partial shielding conditions. The performance of the proposed PV system was verified by

simulation with a detailed switching model in the time domain using the PSCAD/EMTDC software environment.

With the development of PV technology, the PV system integrated buildings have become widely spread. By equipping buildings with PV modules, along with the electricity generation by absorbing solar energy and converting it to electrical energy, the heat that passes in and out of the building through the building envelope can also be reduced. Therefore, the combination of PV modules and building envelope can effectively reduce the building energy consumption, which accounts for 40% of the total energy consumption in the EU and U.S.A (Pérez-Lombard et al., 2008). The PV modules are usually installed on the roof, facade or other parts of a building, such as shading components and PV skylights. Since PV panels are most commonly installed on building rooftop (Oliver and Jackson, 2001), numerous studies on the energy-saving performance of PV rooftop have been conducted.

Dominguez et al. (2011) studied the influence of a PV roof system on building insulation and concluded that during the daytime in the summer season, the temperature of the inner surface of the roof under the PV module was 2.5 K lower than that of the roof without PV modules. Besides, it was found that PV roofs could reduce the annual cooling load by 5.9 $kW \cdot h/m^2$ (38%). Ban-Weiss et al. (2013) presented the installation of integrated PV (BIPV) roofs in Yuma, Arizona, and showed that by using PV modules, the daily average temperature on the roof surface in the summer dropped by 5 °C and the heat transferred into the roof decreased from 1.0 $kW \cdot h/m^2$ to 0.3 ± 0.1 $kW \cdot h/m^2$. Bigot et al. (2009) analyzed the influence of PV roof panels on the heating load of a roof in a humid tropical climate conditions and found that the heating load of the PV roof was reduced by 51% compared with that of a non-PV roof. Ali et al. (2018) evaluated the PV rooftop power generation on Maldives Islands and found that based on the PV-installation areas, the Khurumal Island rooftop PV system could generate 4.8–8.0 GW·h of electricity yearly. In should be noticed that more than 14% of total electricity consumption in Hong Kong was generated by rooftop solar panels (Peng and Lin, 2013), and in Ontario, Canada, rooftop solar panel generated 30% of total electricity consumption (Wiginton et al., 2010). Kapsalis et al., 2014, Kapsalis and Karamanis, 2015 found that in Agrinio, Greece, by using the roof PV panels in the top-floor room, in addition to the power generation, the seasonal heating load increased by 6.7%, and the cooling load decreased by 17.8%. Kotak et al. (2014) compared cooling load of buildings at five key Indian locations using the CIBSE and ASHRAE methods. Their results showed that the cooling load decreased by 73–90% after installing the PV system. In Ref. (Wang et al., 2017), the authors studied the energy-saving caused by the shading effect and power gen

of PV roof by experiments. Salamanca et al. (2016) studied the Phoenix and Tucson and concluded that citywide cooling energy demand could reduce 8–11%. Besides, the overall impact of rooftop PV systems of residential buildings on the energy performance in hot and humid climate conditions was discussed (Dehwah and Asif, 2019). At a roof utilization of 25%, 19% of the overall power demand was offset, and the cooling load was reduced by 2% due to the shading effect of the PV panels.

Besides, some models were developed to calculate heat gain or loss, or heating or cooling load. Shao et al. (2019) used the radiant time-series method (RTSM) to calculate heat gains and cooling and heating load, which denoted a new calculation method for design cooling load calculations. The RTSM differs from the transfer function method (TFM) in both calculating the conduction heat gain and determining the cooling load. Namely, the TFM uses the conduction transfer function to calculate the conduction heat gain transfer function and a room (weighting factor) to determine the cooling load, while the RTSM uses a series of 24 response factors to calculate the conduction heat gain and another series of 24 response factors to determine the cooling load (Spitler and Fisher, 1999).

All the mentioned researches mainly focused on either the power generation capacity of PV systems or the reduction of heat and building load only, without considering the coupling effect between the building and PV system. This coupling effect refers to that when PV modules are attached to the roof, on the one hand, the additional PV modules break the original energy balance of the building envelope and change the heat transfer process, thus causing the change in the heat gain, and cooling and heating loads, further affecting the overall energy consumption of the building. On the other hand, PV modules convert solar energy into electricity providing the power supply to a building, which changes the energy system of the building, also affecting the overall energy consumption form of the building (Ban-Weiss et al., 2013). By ignoring the coupling effect, the energy-saving effect of a PV on the building cannot be determined accurately. Therefore, the main purpose of this work is to develop a comprehensive calculation method of power supply performance and energy-saving performance. Accordingly, the main objectives of this work are as follows: (1) develop a simplified mathematical model to analyze the overall energy-saving mechanism of a PV rooftop; (2) propose a comprehensive energy-saving efficiency theory of a PV roof and introduce an overall energy-saving efficiency index; (3) analyze the adaptability of three PV rooftop types in different regions in China, based on thermal zoning and solar energy resource level zoning.

2. Theoretical analysis

According to the different installation geometries, PV rooftops can be roughly classified into horizontally-mounted, tilted, and firmly-attached to flat and sloping roofs. And in this paper, a horizontally-mounted with sloping roof (Type B), a tilted with sloping roof (Type C), and a PV firmly-attached to a roof (Type D), and the ordinary roof (Type A) that refers to as a reference object would be discussed in this context. It should be noted that there is enough spacing between a PV panels of Type B and a roof so that the roof will not cause overheating. In addition, tracking PV modules are rare in China because of the high price. Therefore, this paper discusses only the PV modules with fixed inclination.

Along with the electricity power generation, solar PV systems generate much heat, which seriously affects the power generation efficiency of the PV systems (Mani and Pillai, 2010). In addition, the PV cells having a high temperature will transfer the heat to the backside of a PV panel, which will affect the temperature and heat flux of the air layer and outer roof surface. On the other hand, due to the shading effect of PV modules, the heat transfer on the roof can be reduced. Hence, PV modules change the heating and cooling loads of a building they are installed on. The electricity generated by PV modules is taken into account when the overall energy-saving effect is calculated. The complete physical analysis model and the thermal process network of a PV rooftop are shown in Fig. 1(a).

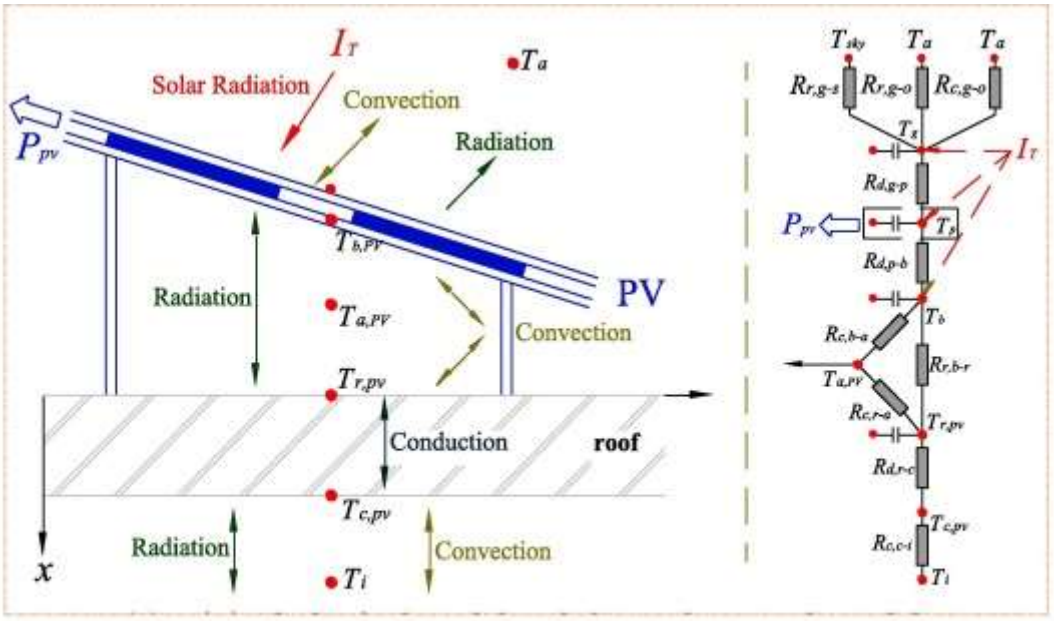

(a) Original physical model and thermal-network model `

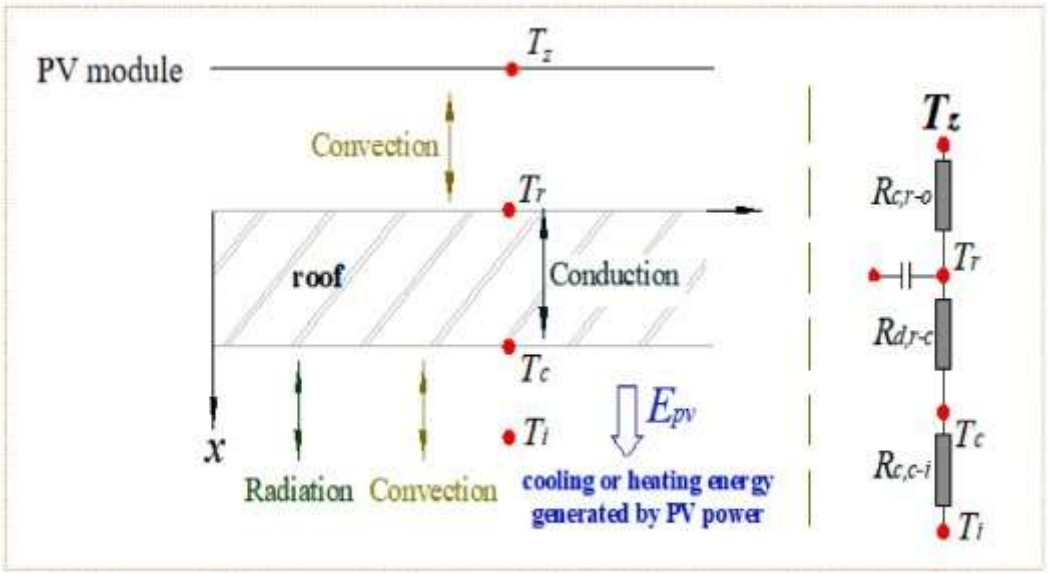

(b) Simplified physical model

Fig. 1. Simplified the PV rooftop physical model.

2.1. Simplified model

The complex theoretical physics model of a roof with a mounted PV panel normally experience the combination of convection, radiation and heat conduction, as shown in Fig. 1(a). However due to the complexity of the model, it is difficult to obtain a universal analytic solution. Therefore, the following assumptions are made for the most widely used rooftop-mounted PV: (1) The heat transfer through the PV modules and the roof is one-dimensional

and has unsteady heat conduction, since the lateral dimensions of the PV modules and roof are much larger than their thicknesses; (2) There is sufficient space between the horizontally-mounted PV modules and a roof to prevent thermal accumulation under the PV modules. Hence, the convective heat transfer boundary layer generated by the high temperature of a PV back panel does not affect the outer surface of the roof; (3) The radiation amount received by a roof from the surrounding buildings is negligible. (4) In the heat transfer model, only the heat transferred to the inner surface of the roof is considered, while the solar radiation and back panel radiation received by the outer surface of the roof and long-wave radiation to the environment are ignored.

According to the assumption (2), the temperature of the air layer above a roof is the same as the ambient air temperature. For a rooftop-mounted PV, the roof heat transfer model presented in Fig. 1(a) can be simplified to the model presented in Fig. 1(b).

The heat transfer process can be expressed as follows:

$$\frac{\partial T}{\partial \tau} = \frac{\lambda_r}{\rho_r C_r}\frac{\partial^2 T}{\partial x^2} \qquad (1)$$

where λr denotes the thermal conductivity of roof material, W/(m·K). ρr denotes the density of roof material, kg/m3. Cr denotes the heat capacity of roof material, J/(kg·K).

The interior surface boundary condition is determined by:

$$-\lambda_r \frac{\partial T}{\partial x}\Big|_{x=\delta} = h_i(T - T_i) \qquad (2)$$

where Ti denotes the indoor air temperature in K, and it is considered constant. hi is the heat transfer coefficient between the internal roof surface and the indoor air in W/(m^2·K). The boundary condition at outer surface for different PV rooftops is given in the following.

Part (a): Roof with a mounted PV

$$-\lambda_r \frac{\partial T}{\partial x}|_{x=0} = h_{c,r-a}(T_{z,pv} - T) \qquad (3)$$

$$T_{\mathrm{Z,PV}}(\tau) = T_a(\tau) + \frac{\alpha_r I_{\mathrm{SDI}}(\tau) + q_{\mathrm{br}}(\tau) - VF \cdot q_{\mathrm{lw}}(\tau)}{h_{\mathrm{c,r\text{-}a}}(\tau)} \qquad (4)$$

where $T_{\mathrm{z,pv}}(\tau)$ denotes the integrated air temperature above PV rooftop in K. $T_{\mathrm{a}}(\tau)$ is the environmental air temperature in K;α_{r} represents the outer surface absorptivity of a roof and it is dimensionless; q_{br} denotes the radiation between the outer surface of the roof and the PV

back panel in W/m^2. The convective heat transfer coefficient of outer roof surface denoted by $h_{c,r\text{-}a}$ can be obtained by the ASHRAE wind speed convection model (ASHRAE, 1997); which means that the convective heat transfer coefficient is determined by the wind speed, and it is defined by Eq. (5). The intensity of the roof incident scattered radiation under shading condition is denoted as I_{SDI}, and it is given by Eq. (6). The long-wave radiation heat dissipation between the outer roof surface and the surrounding environment denoted by q_{lw} could be expressed by Eq. (7).

$$h_{c,r\text{-}a} = e + fV \quad (5)$$

$$I_{SDI} = I_{DI} \cdot VF \quad (6)$$

$$q_{l_w} = \varepsilon_r \sigma_b [F_a({T_r}^4 - {T_a}^4) + F_{s_{ky}}({T_r}^4 - {T_{s_{ky}}}^4) + F_{g_r}({T_r}^4 - {T_{g_r}}^4)] \quad (7)$$

In Eqs. (5), (6), (7), e and f represent the wind speed coefficients, and their values are taken from Ref. (Palyvos, 2008); I_{DI} denotes the intensity of roof incident scattered radiation in the absence of shading in W/m^2; VF and εr denotes the view factor and the roof surface emissivity, and they are both dimensionless; F_a, F_{sky} and F_{gr} denote the radiation angle coefficient between the outer roof surface and the ambient air, sky and ground respectively, dimensionless quantities; T_r denotes the temperature of the outer roof surface in K; T_{gr} represents the ground temperature in K, and lastly σ_b is the Stefan-Boltzmann constant.

Back panel temperature of PV panels denoted by T_b can be obtained from the empirical formula for the back temperature of PV modules in the Sandia electrical performance model developed by Sandia National Laboratory (Davis et al., 2001).

$$T_b(\tau) = T_a + I_T \cdot exp(a + bV) \quad (8)$$

In Eq. (8), the empirical coefficients a and b are −3.562 and-0.07862, respectively; V denotes the wind speed in m/s. The sky temperature could be obtained by the following formula (Duffie et al., 1980).

$$T_{sky} = 0.0552 T_a^{1.5} \quad (9)$$

Part (b): Roof with a firmly-attached PV

$$-\lambda_r \frac{\partial T}{\partial x}\Big|_{x=0} = h_{c,r-a}(T_{zm} - T) \quad (10)$$

$$T_{zm}(\tau) = T_a(\tau) + \frac{\alpha_c I_T - q_w(\tau)}{h_{c,g-a(\tau)}} \quad (11)$$

where T_{zm} denotes the integrated air temperature in K, $h_{c,g\text{-}a}$ denotes the convection heat transfer coefficient of a glass cover plate in W/(m^2·K), I_T denotes the total incident radiation intensity in W/m^2; α_C represents the absorptivity of PV battery pack, a dimensionless quantity. $q_w(\tau)$ denotes the radiation heat transfer between the outer roof surface and the surrounding environment of PV panels in W/m^2.

Part (c): Ordinary roof

$$-\lambda_r \left.\frac{\partial T}{\partial x}\right|_{x=0} = h_{c,r\text{-}a}(T_{zc}-T) \quad (12)$$

$$T_{ZC}(\tau) = T_a(\tau) + \frac{\alpha_r I_T(\tau) - q_{lw}(\tau)}{h_{c,r\text{-}a}(\tau)} \quad (13)$$

where T_{zc} denotes the integrated air temperature of an ordinary roof in K; αr denotes the absorptivity of the outer roof surface, and it is dimensionless; $q_{lw}(\tau)$ denotes the radiation heat transfer between the outer roof surface and the ambiance environment in W/m^2.

2.2. Solving methods

In order to analyze the influence of shading on roof heat gain under the temperature boundary conditions, the periodic response factor (PRF) discrete methods is chosen to calculate the conduction heat gain as a function of time. Next, the radiation time factor (RTF) methods is used to convert heat gain into cooling or heating load. The hourly heat gain is calculated by:

$$q_\theta = A\left(\sum_{j=0}^{23} Y_j t_{Z,\theta - j\Delta\tau} - t_i \sum_{j=0}^{23} Y_j\right) \quad (14)$$

where Y_j stands for the PRF for a period of 24 h, $t_{Z,\theta\text{-}j\Delta\tau}$ denotes the sol-air temperature j hours ago in K, Δτ is the time interval, and here, it is set to1 h, and lastly, A is the roof area in m^2.

The total heat gain transferred to the interior is divided into radiation and convection gain contributions. The heat gained by the convection is directly converted into the convection cooling load, whereas the heat gained by the radiation is converted into the radiation cooling load using the RTF. For the roof, the radiation and convection components account for 0.84 of the total heat gains and the remaining 0.16 were due to convection (Spitler and Nigusse, 2010). The hourly cooling load of a roof is given by:

$$Q_\theta = 0.84\sum_{j=0}^{23} r_j \cdot q_{\theta - j\Delta\tau} + 0.16 q_\theta \qquad (15)$$

where r_0, r_1, …r_{23} denote the RTFs representing the current proportions of the heat gain to the cooling load, and they are dimensionless, while $q_{\theta\text{-}j\Delta\tau}$ denotes the conduction heat gain hours ago, respectively. The solving procedure presented in this research is shown in Fig. 2.

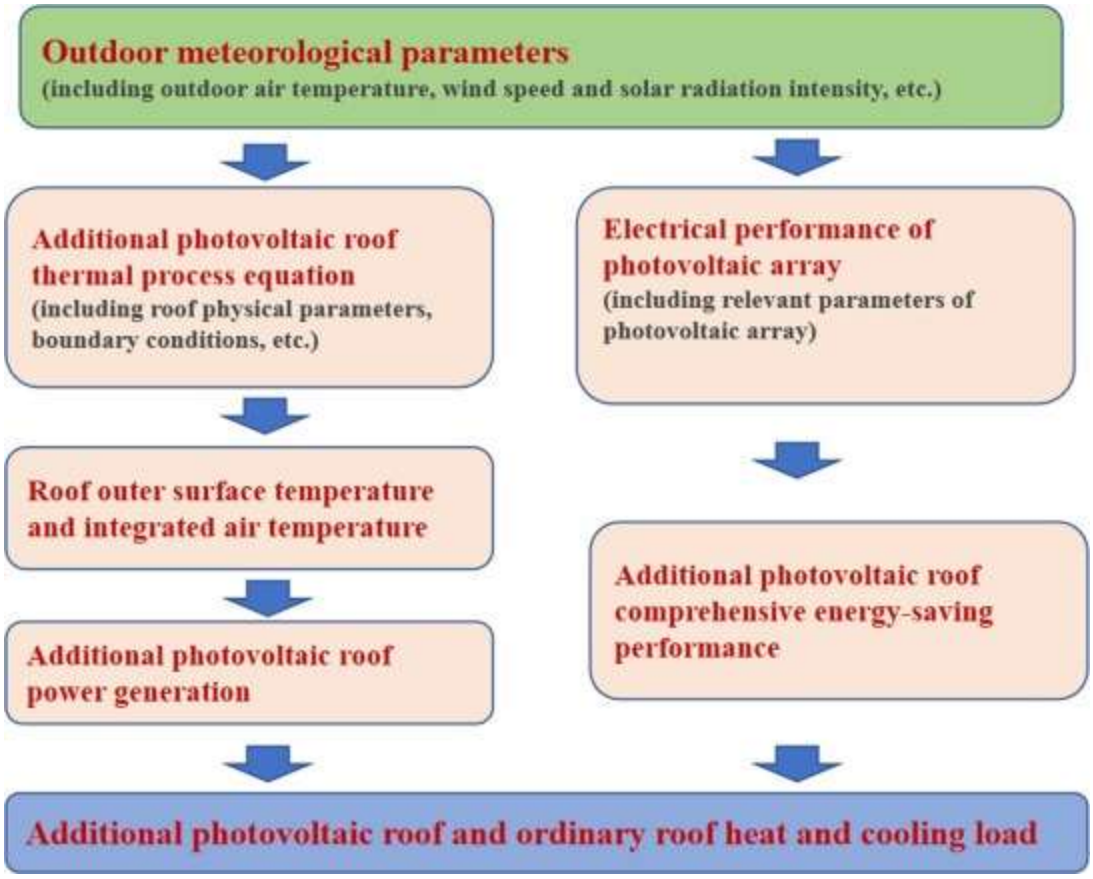

Fig. 2. Calculation flow chart of the overall energy saving performance of PV roof.

First, weather data, including the irradiance, ambient temperature and wind speed are fitted, and the thermal property parameters of the roof and PV modules are determined. Next, a piecewise one-dimensional unsteady heat transfer model is established using COMSOL software, the thermal boundary conditions are input parameters in the form of variables to calculate the roof surface temperature, and then the comprehensive air temperature above the roof is obtained. By substituting the comprehensive air temperature into the Eqs. (14) and (15), the indoor heat gain (heat loss) and heating (cooling) load of the roof can be obtained, respectively. At the same time, the electrical performance system diagram is established by TRNSYS software to obtain the power generation of PV modules. The obtained cooling (heating) load is substituted into the Eq. (16) to obtain the shading gain. The

generated power value is substituted into the Eq. (17) to obtain the power gain. Then the shading gain and the power gain are substituted into the Eq. (18) to obtain the comprehensive energy-saving efficiency of the PV rooftop.

2.3. Overall energy-saving evaluation index

The benefits of a PV mounted on top of the roof can be divided into shading gain and power generation based on the cost-saving and income-increasing advantages. The daily shading gain of PV panels can be calculated by.

$$Q_{\mathrm{z}} = \sum_{\theta=0}^{23} (Q_{\mathrm{n}\theta} - Q_{\mathrm{PV}\theta}) \qquad (16)$$

where $Q_{\mathrm{n}\theta}$denotes the hourly cooling or heating load of a roof without PV panels given in W, and $Q_{\mathrm{pv}\theta}$ denotes the hourly cooling or heating load of PV rooftop, W.

The power generation of the PV rooftop can be obtained by converting the hourly power generation of the PV module into cooling or heating load according to a certain COP. The daily power generation of a PV rooftop E_{pv} can be expressed as:

$$E_{\mathrm{pv}} = \sum_{\theta=0}^{23} P_{\mathrm{PV}\theta} \times COP \qquad (17)$$

where $P_{\mathrm{pv}\theta}$ denotes the generated power of a PV rooftop at θ moment in W, and COP represents the performance coefficient of an air conditioning system.

After obtaining the comprehensive effect of a PV rooftop on the building energy consumption, in order to facilitate the comparison with an ordinary roof and promote application, the overall energy-saving efficiency index of a PV roof denoted as η_{sys} is introduced, and it is expressed as:

$$\eta_{\mathrm{sys}} = \frac{E_{\mathrm{pv}} + Q_{\mathrm{z}}}{I_T} \qquad (18)$$

In the following sections, the overall energy-saving efficiency η_{sys} is utilized to analyze specific energy-saving effects in different regions of China in subsequent sections.

2.4. Experimental setup

In order to validate the simplified model, an experiment was conducted in the period from October 2016 to November 2016. Three 260-W PV panels were horizontally, tilted and

attached installed on the rooftop, respectively. A 20 cm gap was kept between the horizontal PV panels and the roof. The tilted PV array was installed facing South at the inclination angle of 30°. The building with an accessible roof used in the experiment is in the Shaanxi province, in China.

During the experiment, the temperatures of the cover plate, back panel of the polysilicon PV panel, the air interlayer, and inner and outer surfaces of the roof were measured. The incident solar radiation intensity, outdoor air temperature, and wind speed on the roof surface were also measured. The parameters of the equipment used in the experiment are given in Table 1, and the pictures of experimental PV roofs and devices used in the experiment are displayed in Fig. 3.

Table 1. Parameters of the measurement instruments.

Parameter	**Sensor type**	**Range**	**Accuracy**
Cover plate temperature	CENTER309 Thermocouple	−200 °C to 200 °C	±(0.3% value) +1 °C
Back panel temperature of PV			
Air interlayer temperature	iButtonDS1922L/TR-72wf	−20 to 85 °C; 0–100%/0–55 °C	±0.5 °C
Inner surface temperature of the roof			
Outer surface temperature of the roof	CENTER309 Thermocouple	~200 °C to 200 °C	±(0.3% value) +1 °C
Incident solar radiation intensity	Solar power generation test recorder	Radiation: 0–2000 W/m^2 Wind speed: 0–60 m/s	±5%
outdoor air temperature	iButtonDS1922L/TR-72wf	−20 to 85 °C; 0–100%/0–55 °C;	±0.5 °C
wind speed	Solar power generation test recorder	Radiation: 0–2000 W/m^2	±(0.3 + 0.03 V) m/s

Parameter	Sensor type	Range	Accuracy
		Wind speed: 0–60 m/s	

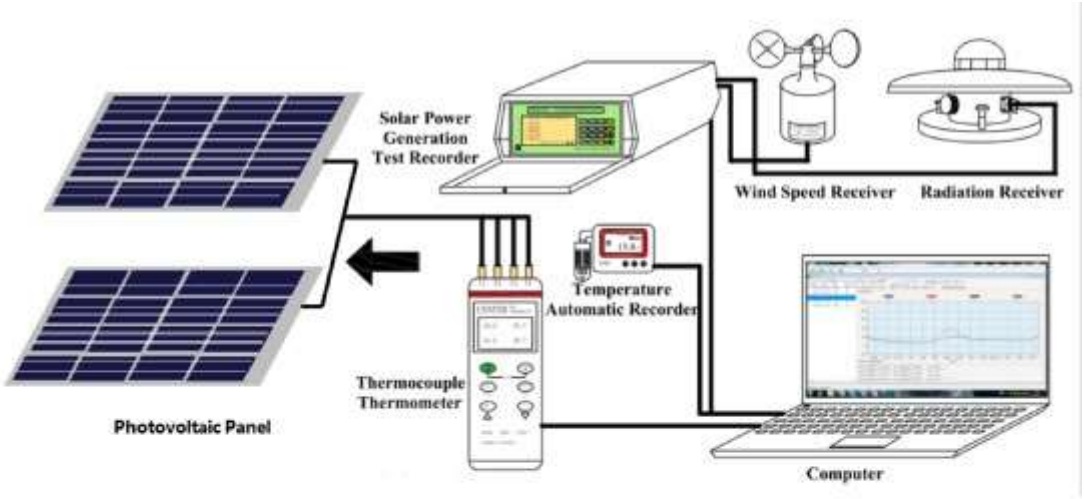

(a) Experimental principle diagram

a. Horizontally-mounted PV roof b. Tilted PV roof c. Firmly-attached PV roof

(b) Three types of roof mounting rooftop PV panels

Fig. 3. The schematic diagram of the experimental apparatus.

The surface and air temperatures of the PV rooftop were measured during the experiment, and the heating and cooling loads were obtained by the above-presented calculation methods using the measured data. The obtained results are given in the following three sections.

2.5. Uncertainty analysis

In order to illustrate the influence factors to the overall energy-saving efficiency, the test data were analyzed using SPSS 26.0. The Analysis of Variance (ANOVA) was used to determine whether a particular variable had a significant influence on the overall energy-saving efficiency. The significance level was set to 0.05, which meant the results were statistically significant when the $P < 0.05$. The analysis results showed that the influences of the air temperature and horizontal total solar radiation on the overall energy-saving efficiency were significant, while the wind speed was not. The results are given in Table 2, Table 3.

Table 2. ANOVA.[a]

Model	Quadratic Sum	DOF	Mean Square	F	Significance
Regression	0.221	4	0.055	39.975	0.000[b]
Residual	0.029	21	0.001		
Sum	0.250	25			

a Dependent variable: Overall energy-saving efficiency.

b Independent variable: Wind speed, Air temperature, Horizontal total solar radiation.

Table 3. Coefficient.[a]

Model	Unstandardized coefficient		Standardized coefficient	t	Significance	Confidence interval (95%)	
	B	Standard error	Beta			Lower limit	Upper limit
Air temperature	−0.005	0.001	−0.698	−4.185	0.000	−0.007	−0.002
Horizontal total solar radiation	0.000	0.000	−0.274	−2.402	0.026	−0.001	0.000
Wind speed	0.000	0.007	−0.001	−0.019	0.985	−0.14	0.014

a Dependent variable: Overall energy-saving efficiency.

3. Experimental results and model validation

3.1. Experimental verification of proposed model

In order to examine the consistency between the theoretical and the experimental results, and to verify the accuracy of the proposed model, the Mean Relative Error (MRE) and Percent Accuracy Error (PAE) indexes were selected as evaluation metrics, and they were calculated by:

$$MRE = \frac{1}{n}\sum_{i=1}^{n}\frac{|C_i - M_i|}{M_i} \quad (19)$$

$$PAE = 1 - \frac{\frac{1}{n}\sum_{i=1}^{n}|C_i - M_i|}{\overline{M}} \qquad (20)$$

where C_i denoted the simulation result and M denoted the experimental result. r was the variable number.

The hourly temperature of the outer surface of the PV roof for different configurations obtained by the COMSOL calculations was compared with measured data from experiment, as shown in Fig. 4. In Fig. 4, it can be seen that the theoretical values were in good agreement with the experimental values since the hourly temperature error was within 10% in general. The reason for these errors can be explained by the fact that, the roof was relatively humid and covered with dusts, which made the heat transfer coefficient, density, specific heat capacity and thermal inertia index of the experimental roof different from the calculated values. The results showed that the mean relative errors (MRE) of horizontally-mounted PV roof, tilted PV roof, attached PV roof, and ordinary roof were 4.10%, 3.77%, 5.67%, and 3.38% respectively, and the corresponding percent accuracy errors (PAE) were 96.2%, 95.6%, 94.6%, and 97.6%, respectively. In conclusion, the simplified calculation model of the roofs with three types of PV mounting was very accurate.

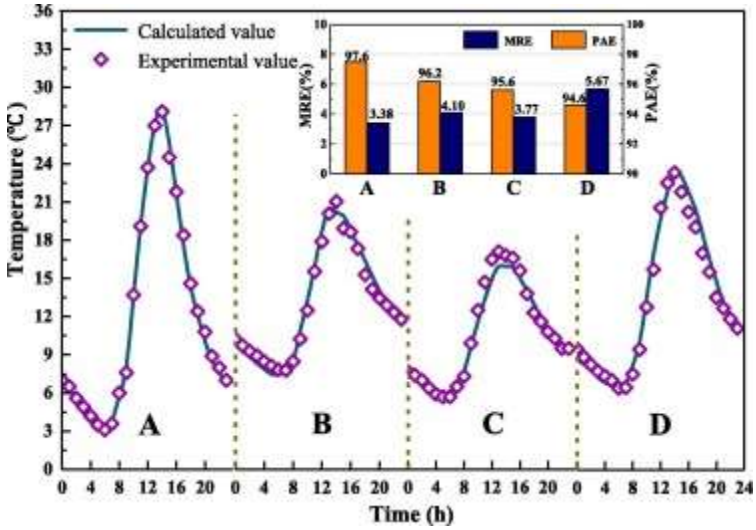

Fig. 4. Comparison between the experimental results and theoretical calculation results (A-ordinary roof; B- horizontally-mounted PV roof; C-tilted PV roof; D-firmly-attached PV roof).

3.2. Surface and air temperature results

The roof type in ASHRAE was selected for both the experiment and the calculation due to its simple structure, which is convenient for modeling after adding PV modules (Wang et al.,

2006). Photowatt (PW) l000 was selected as a PV module. See Appendix A for details on PV modules and roof structures.

In addition to the parameters of the roof and PV modules, some variables and empirical parameters used in the calculation are listed in Appendix B.

In the experiment, the outer surface temperature, integrated air temperature and heat gain of the roofs were obtained, along with the cooling and heating load of the building.

Due to the shading effect, the outer surface temperature and integrated temperature of the roofs with PV (Types B, C, and D) were lower than those of the ordinary roof (Type A), as shown in Figs. 5 and 6. Among all the studied configurations, the tilted PV roof showed the most significant shading effect. This was because this roof type had a lower angle coefficient between the PV back panel and roof surface than the other roof types. Moreover, an effective temperature of the night sky is much lower, which facilitates the heat exchange between roof and the sky. Under such circumstances, the PV modules reduced the heat dissipation from the long-wave radiation outward from the roof, thereby providing insulation for the roof system. Therefore, the surface temperature at night of the PV rooftop was generally higher than that of the ordinary roof, and the effect of horizontal overhead PV roof is more obvious. Furthermore, the trends of outer surface temperature and the integrated air temperature of the attached PV roof were close to those of the ordinary roof. This was mainly because the upper surface of the control body of the attached PV module received all solar radiation, just like the ordinary roof. However, due to the high temperature of the glass cover of the PV module, it emitted more long-wave radiation to the surrounding environment than the ordinary roof, so the integrated air temperature was slightly lower than that of the ordinary roof. Moreover, the presence of a closed air interlayer increased the overall thermal resistance of the control body, but at the same time the air interlayer was too thin to achieve complete insulation, so the highest outside surface temperature of the attached additional PV roof was lower than that of the horizontal overhead PV roof, but higher than that of the ordinary roof. At the same time, the lowest outside surface temperature of attached additional PV roof was higher than that of the ordinary roof but slightly lower than that of horizontal overhead PV roof. Finally, Fig. 6 also shows that the maximum temperature difference between the three PV roofs and the ordinary roof was about 12 °C, and the peak temperature appeared 2 h later.

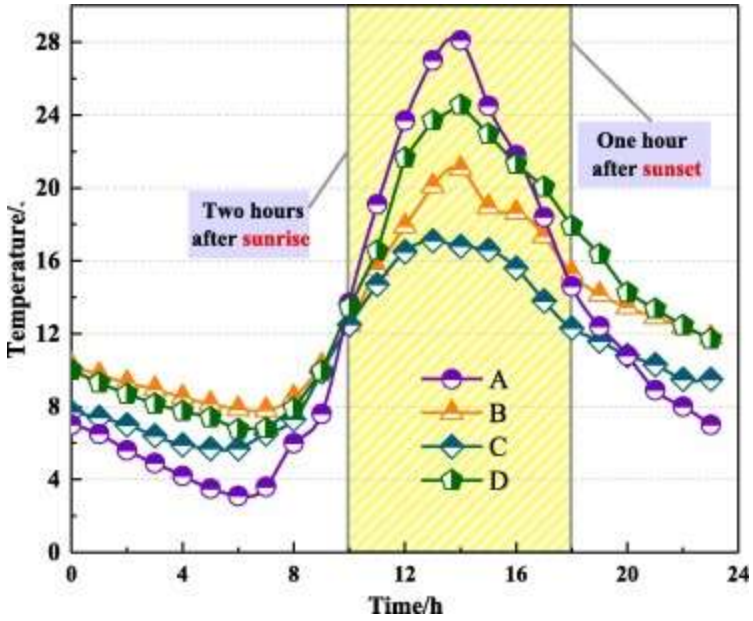

Fig. 5. The outer surface temperature for roof types (A-ordinary roof; B- horizontally-mounted PV roof; C-tilted PV roof; D-firmly-attached PV roof).

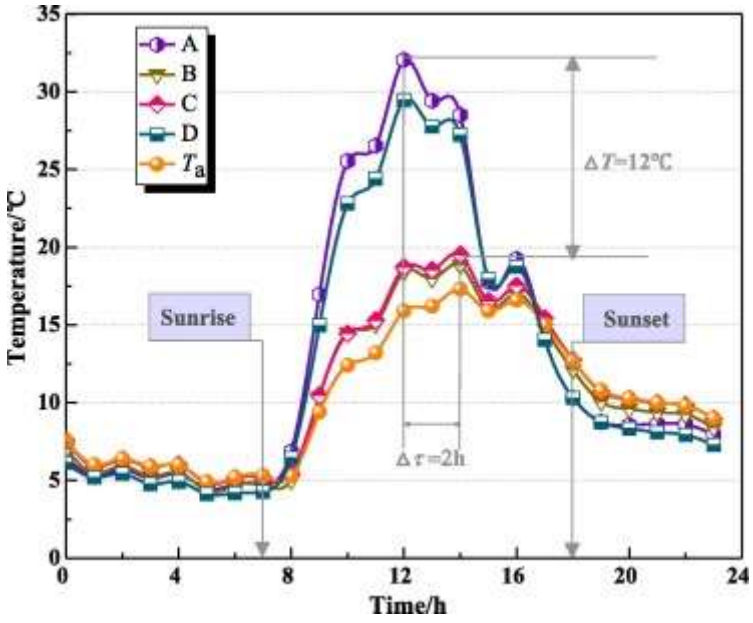

Fig. 6. Integrated air temperature for different roof types (A-ordinary roof; B-horizontally-mounted PV roof; C-tilted PV roof; D- firmly-attached PV roof).

3.3. Heating and cooling load results

The shading effect of the PV modules on the heat gain of the roofs is shown in Fig. 7, and the effect of PV modules on the heating and cooling load is presented in Fig. 8. Compared with the ordinary roof, the heat gain caused by the short-wave solar radiation of the PV roofs was sheltered, and the heat loss caused by the PV roof's long-wave radiation was reduced. For these reasons, both the heat gain and the cooling load per unit area of the PV roofs were

significantly reduced, but the heating load increased, and the fluctuation range was relatively small. The firmly-attached PV roof had a much smaller decrease in cooling load and heat gain than the other two PV roof types. The reason was that the PV modules attached to the roof increased the roof structure and thermal resistance of the PV modules and closed air layer, but did not reduce the heat as much as to cut the heat input directly as the overhead PV roof did.

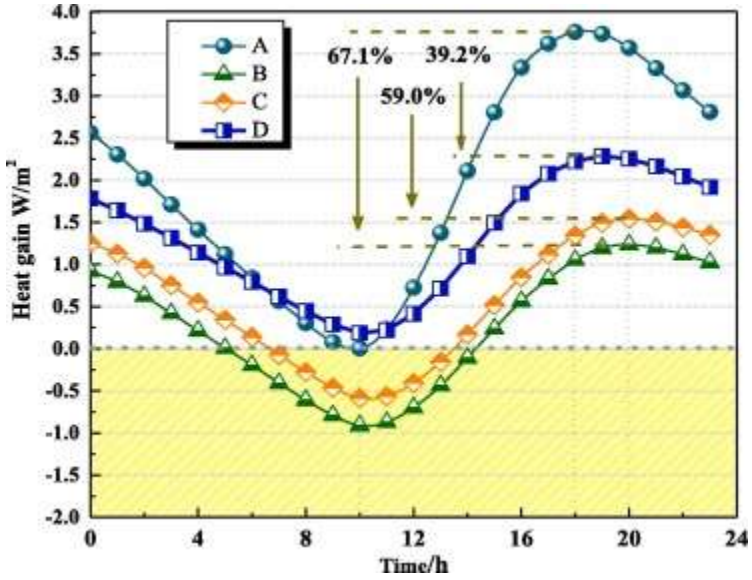

Fig. 7. Heat gain of different roof types (A-ordinary roof; B- horizontally-mounted PV roof; C-tilted PV roof; D- firmly-attached PV roof).

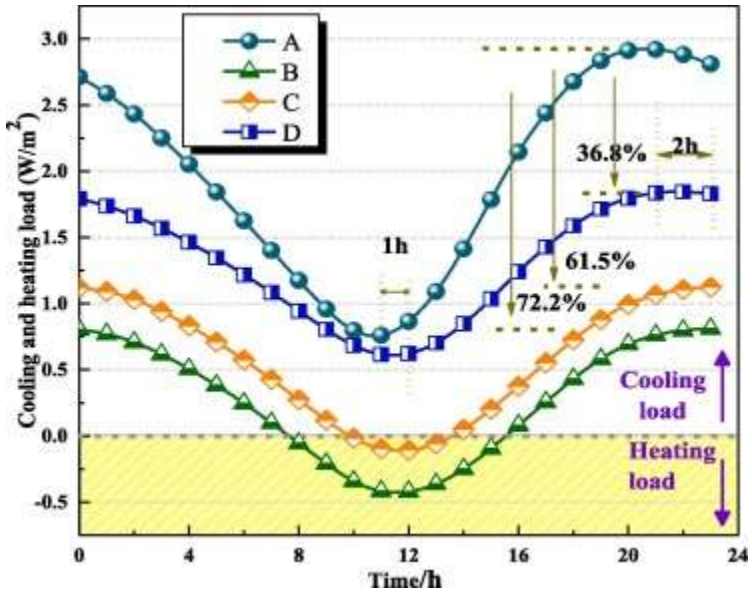

Fig. 8. Heating and cooling load of different roof types (A-ordinary roof; B-horizontally-mounted PV roof; C-tilted PV roof; D- firmly-attached PV roof).

Compared with the ordinary roof, the peak values of the heat gain of the horizontally-mounted PV roof, tilted PV roof and attached PV roof were reduced by 67.1%, 59.0%, and

39.2% respectively, and the total daily heat gain values decreased by 86.5%, 70.6%, and 33.7%, respectively. The peak cooling load and the total daily load of the horizontally-mounted overhead PV roof decreased by 72.2% and 77.4%, of the tilted overhead PV roof decreased by 61.5% and 69.4%, and of the attached PV roof decreased by 36.8% and 33.7%, respectively. Due to the shielding effect on the roof, the heat storage capacity of the PV roofs was changed. Compared to the ordinary roof, the peak cooling loads of the horizontally-mounted PV roof and tilted PV roof were delayed for 2 h, and the peak heating loads were delayed for 1 h. There was also a delay in attaching PV roofs, but it was not obvious.

The detailed information on the average energy-saving ability of the different PV roof types is shown in Fig. 9.

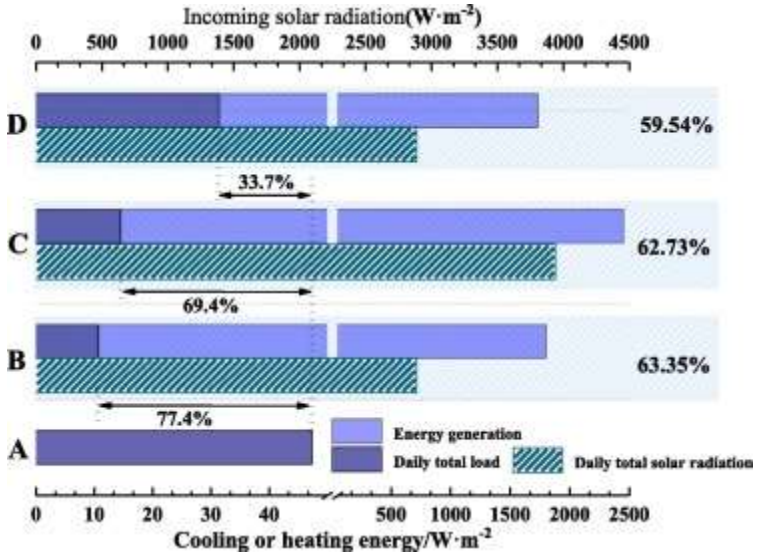

Fig. 9. The average energy-saving ability of different PV roof types (A-ordinary roof; B- horizontally-mounted PV roof; C-tilted PV roof; D-firmly-attached PV roof).

Due to the shading benefit, the total daily loads of the horizontally-mounted PV roof, tilted PV roof, and firmly-attached PV roof were reduced by 77.4%, 69.4%, and 33.7%, respectively, as compared to the ordinary roof. Considering the double-effect of shading benefit and power generation, the daily overall energy-saving efficiency of the horizontally-mounted PV roof, tilted PV roof, and firmly-attached PV roof were 63.35%, 62.73%, and 59.54%, respectively.

4. Analysis and discussions of overall energy-saving performance

The overall energy-saving efficiency of a PV roof is affected by both outdoor air temperature and solar energy resources. Therefore, by integrating the building's thermal engineering zoning provided by the Thermal Design Code for Civil Building (Spitler and Nigusse, 2010)

and solar energy resources distribution of China, 13 respective cities in China were selected as the research objects, as shown in Fig. 10. Locations and climate conditions of these cities are shown in Fig. 10 and Appendix C.

Fig. 10. Selected 13 cities on the map of China.

4.1. Cooling/heating load analysis

In areas such as Golmud, Xining, and Lhasa, there are strong solar radiation and large diurnal range, so the building with horizontally and tilted mounted PV can achieve a significant reduction in daily heat gain and cooling load in summer, as shown in Fig. 11 and Fig. 12, respectively. Compared to the ordinary roof, the heat gain decrease, and the cooling load reduction of the PV roof reached 0.5 MJ/m^2 and 12 W/m^2, respectively. On the other hand, in areas with the small daily temperature diurnal range and high average temperature that have hot summers and warm winters, such as Guangzhou and Sanya, although the peak cooling load of the PV roofs was slightly reduced, the total daily heat and cooling loads were higher than those of the ordinary roofs. In other words, PV modules increased the cooling load of buildings in Guangzhou and Sanya.

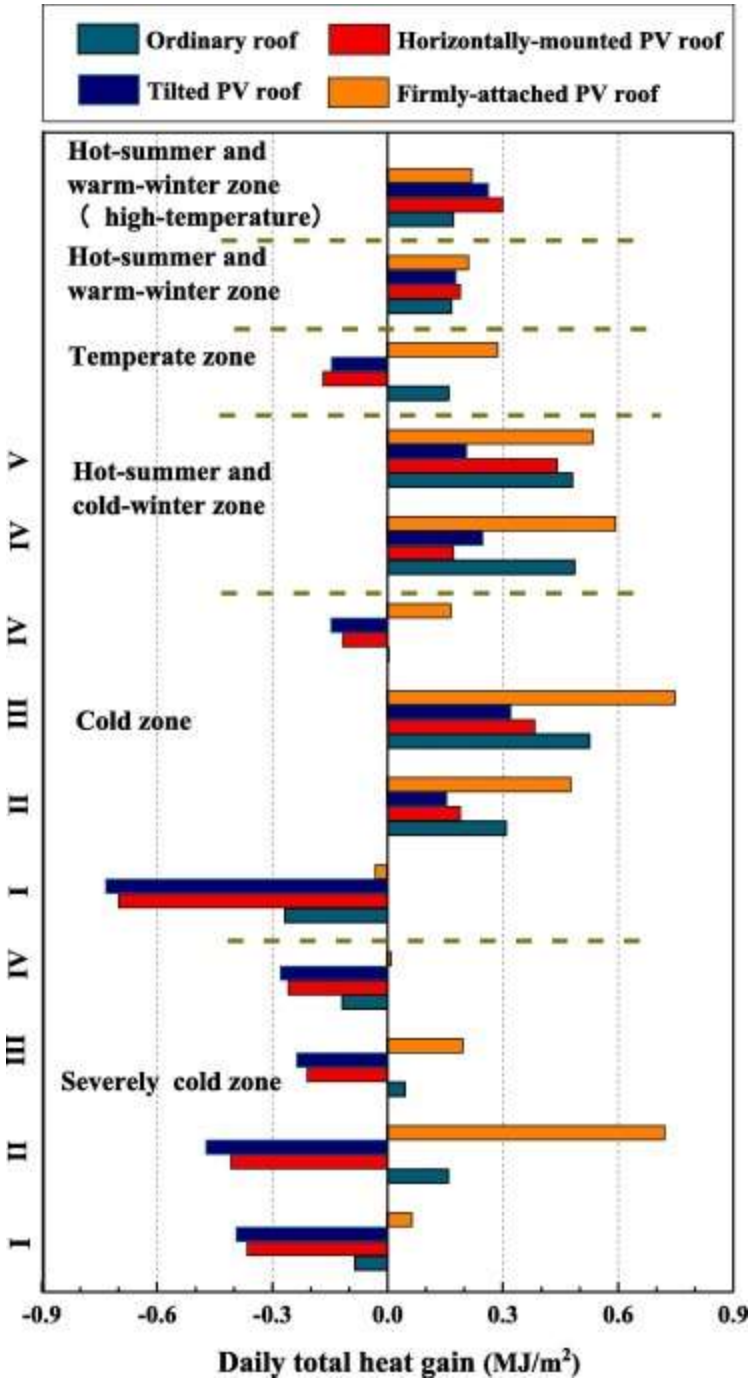

Fig. 11. Typical daily total heat gain in summer.

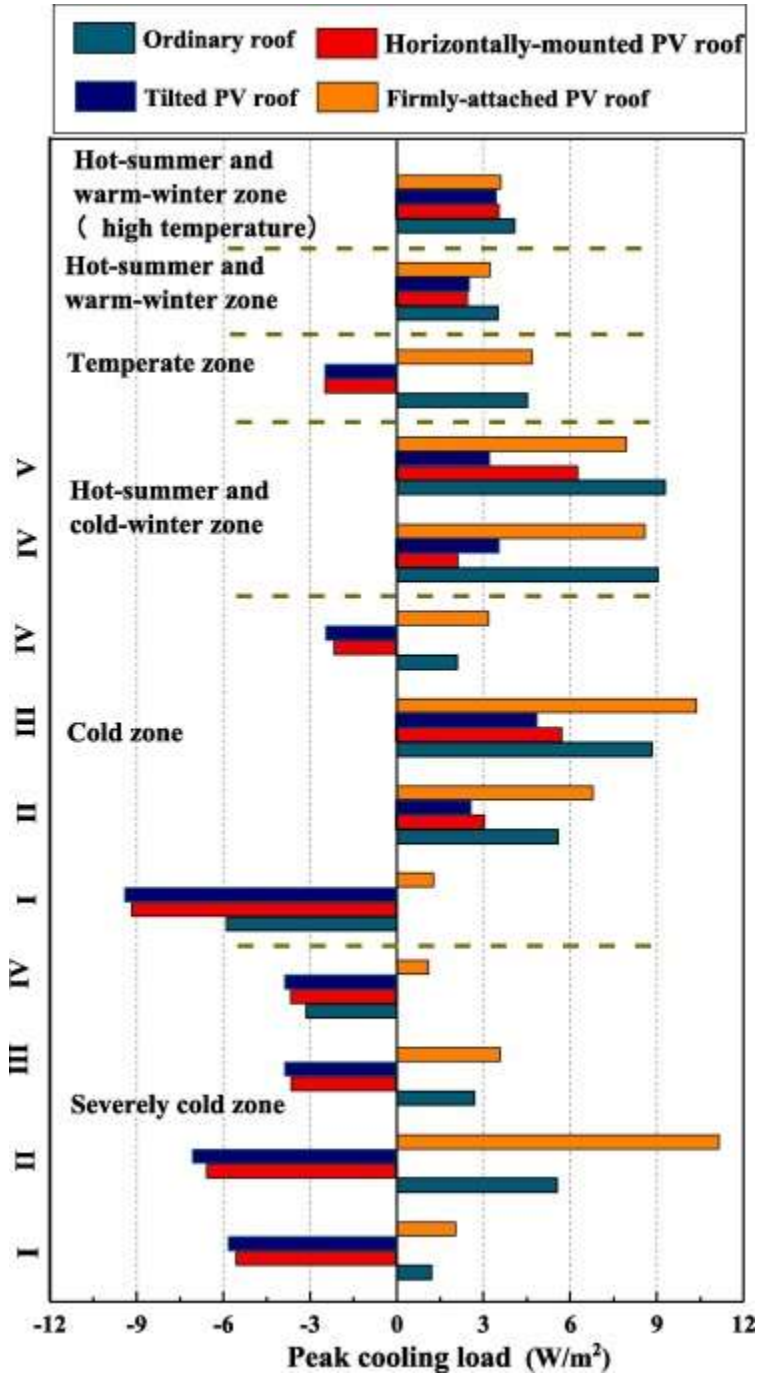

Fig. 12. Typical Peak cooling load in summer.

Based on these results, when PV roofs are used in areas with the small daily temperature diurnal range and the higher average temperature in summer, placing the roof at sunrise and removing it at night can maximize the energy-saving effect, because of better heat dissipation at night. Obviously, this conclusion is drawn from the academic point of view, but the practicability should also be considered during the implementation.

The typical daily total heat loss and the peak heating load of different roofs in the winter season are shown in Fig. 13 and Fig. 14, respectively.

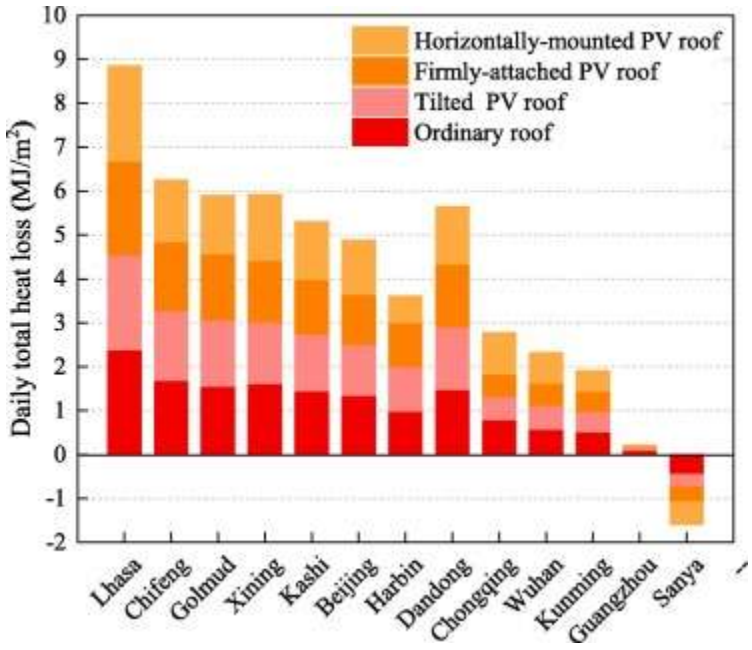

Fig. 13. Typical daily total heat loss of different PV roof types during the winter.

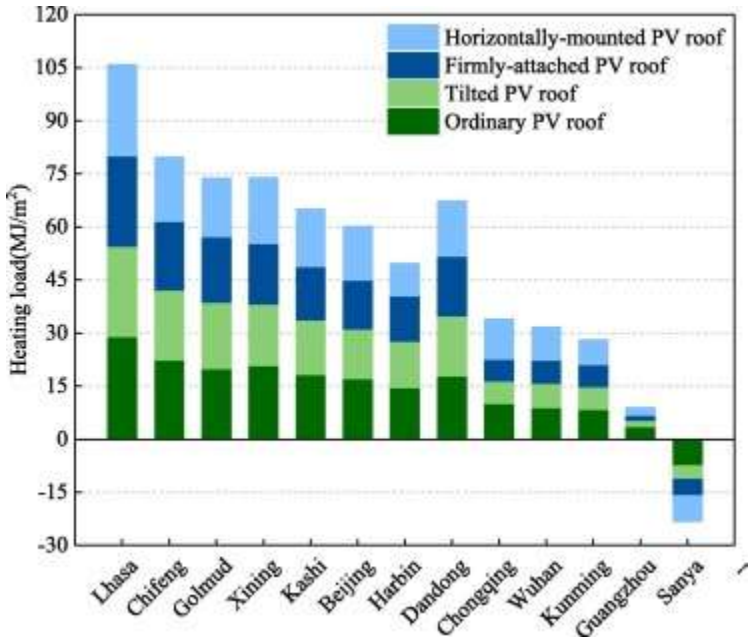

Fig. 14. Typical peak heating load of different PV roof types during the winter.

As shown in Fig. 13, Fig. 14, the total daily heat loss and the peak heating load corresponding to the roofs with horizontally and tilted mounted PV modules were generally reduced in the winter season for all the cities, except for Lhasa. The total heat loss and the peak heating load were reduced by nearly 0.3 MJ/m^2 and 4 W/m^2, respectively. However, the heating load of the overhead PV roof was higher than that of the ordinary roof after about 16:00 in some of the cities. This was because the solar radiant heat received by the ordinary roof could be transmitted into the building at noon, which could further reduce the heating load in this period. The load fluctuation range of the overhead PV roof was small due to the effect of PV

modules on the long-wave radiation dissipation on the roof at night and the reduction of solar radiation during the day, which reduced the daytime heat gain and heat loss on the roof at night. In addition, the daily total heating load of the tilted overhead PV roof was slightly higher than that of the horizontally-mounted overhead PV roof, which was opposite to the cooling load in the summer season. Thus, a tilted overhead PV roof is more suitable for the summer season and a horizontally-mounted overhead PV roof is more suitable for the winter season.

In areas with hot summer and cold winter, the daily total heat loss and the peak heating load of the firmly-attached PV roof are higher than those of the ordinary roof. This is because, in such regions, winter temperature is relatively high, the radiation intensity is low, the solar heat difference absorbed by PV modules and roof is small, and the temperature difference between the PV cell components and roof surface is large. Therefore, integrated air temperature of the firmly-attached PV roof is lower than the ordinary roof, which in turn causes its surface heat loss to be greater than that of the ordinary roof, so its total daily heating load is high.

4.2. Overall energy-saving efficiency evaluation

The overall energy-saving efficiency of a PV roof of the selected cities in the summer season is shown in Fig. 15. As presented in Fig. 15, the shading benefit and power generation were superimposed. The shading benefit of the overhead PV roof was positive except in the hot-summer and warm-winter areas. In these areas, the shading benefit of the tilted PV roof was better than that of the horizontally-mounted PV roof, while the attached type was negative except for Chongqing, which had lower solar radiation. It was also observed that for almost all the areas, the attachment type installation was not suitable during the summer. In addition, although the solar radiation was high in the hot-summer and warm-winter area, the comprehensive shading benefit was negative, which was due to the overall higher air temperature during the day and night and lower temperature difference. As a result, the shading effect of the PV module on the long-wave radiation of the roof was stronger than the shielding effect of the heat of the incident radiation.

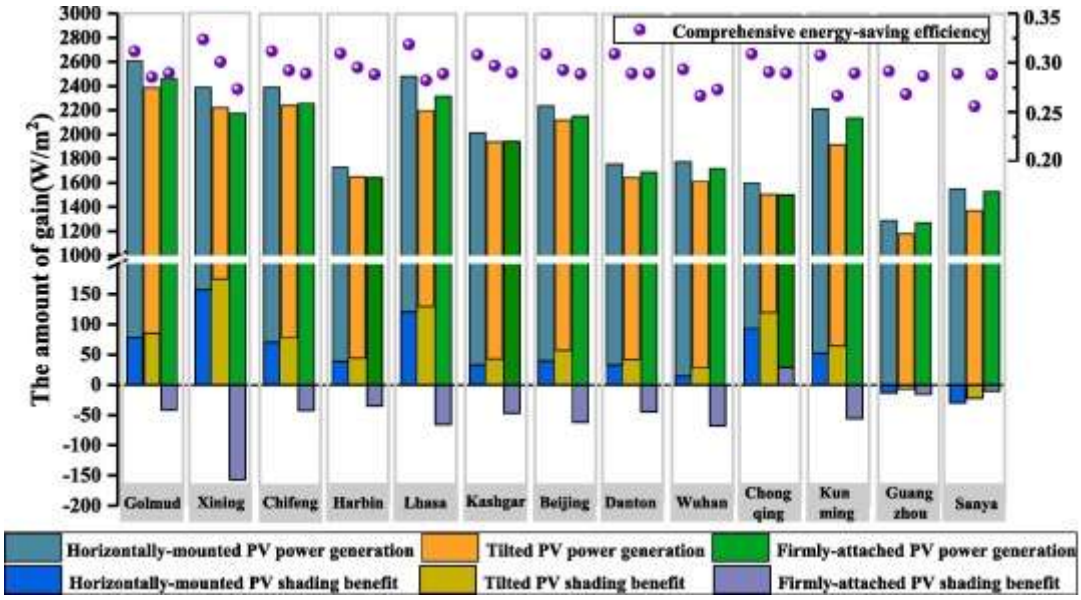

Fig. 15. The overall energy-saving efficiency of studied cities in the summer.

The overall energy-saving efficiency results in Fig. 15 show that the efficiency was in the range of 0.25–0.35. The overall energy-saving efficiency of the horizontally-mounted PV roof was the highest, with a value of 0.32. Although the inclined type had a stronger effect on load reduction in the summer, the total solar radiation intensity incident on the horizontal plane was higher than that of the inclined plane. Therefore, the generation capacity of the horizontally-mounted PV module was greater than that of the inclined type.

In summary, a horizontally-mounted PV roof is more suitable in the summer. When possible, in the hot-summer and warm-winter areas, PV modules should be removed at night so that the roof can radiate the long-wave radiation to the environment, thereby making the shading benefit positive.

The overall energy-saving efficiencies of the selected cities in the winter are shown in Fig. 16. As displayed in Fig. 16, in all the cities except for Guangzhou and Sanya, the shading benefit of the PV module in all cities was positive, and the heating load was reduced to a certain extent. It meant that the reduction in heat dissipation due to the long-wave radiation and heat radiation between the back-plate of PV modules and the roof was better than that of PV modules solar radiation heat reduction. Also, the heat insulation of the PV modules was stronger than the shading effect. Contrary to the observations in the summer, the shading benefit of the horizontally-mounted PV roof was higher than that of the tilted PV roof. This was because the radiation angle coefficient facilitated better insulation.

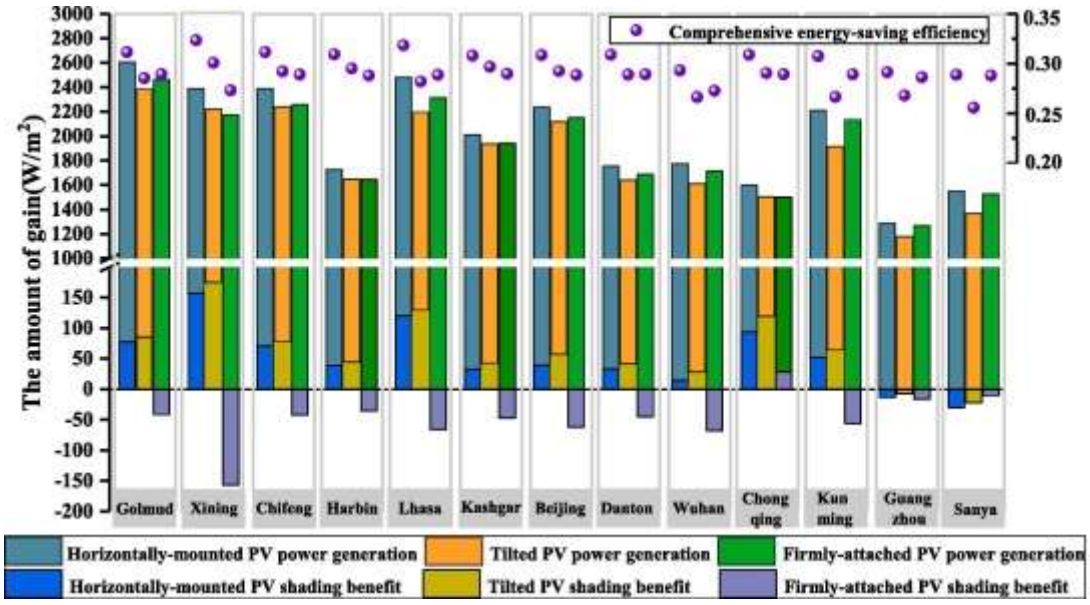

Fig. 16. The overall energy-saving efficiency of studied cites in the winter.

In addition, the overall energy-saving efficiency of the studied cities in winter was quite different from those of Golmud to Sanya, which was due to the lower power efficiency of the modules at higher temperatures. Except for Chongqing, in all other cities, the overall energy-saving efficiency of the tilted PV roof was higher, while the difference between the horizontally mounted and the firmly-attached PV roof was small, the solar radiation of the inclined plane was higher than that of the horizontal plane, and power generation of the tilted PV roof was higher than those of the other PV roof types. Although the total solar radiation was greatly reduced in the winter, the efficiency of the PV modules was higher at lower ambient temperatures. Therefore, in the winter, the overall energy-saving efficiency was up to 0.97, and it was higher than that in the summer. In conclusion, the tilted PV roofs are more suitable for the winter season, and in cold and severely cold regions, where the temperature difference between day and night is large, and the average temperature is low, the overall energy-saving efficiency is relatively high.

There is a difference between the suitable roofs for the summer and winter seasons; namely, in the summer, the total solar radiation intensity on the horizontal surface is higher than that on the sloping surface. Considering the shading effect only, compared to the tilted overhead PV roof, the radiation between the horizontally-mounted PV panels and the roof is stronger, and heat gain through the roof is larger, but the power generation of the horizontal overhead PV modules is much larger than that of the tilted PV roofs. On the other hand, in the winter, the solar radiation on the inclined surface is higher than that on the horizontal surface, compared to the horizontally-mounted overhead PV roof, the tilted overhead PV roof obtained heat more. Although it could increase the radiation dissipation at night. The power

generation of the tilted overhead PV roof is much higher than those of the other two PV roof types. Therefore, by considering both the shading and the power generation effects, a horizontally-mounted overhead PV roof is more appropriate for the summer, while a tilted overhead PV roof is more suitable for the winter.

5. Conclusions

In order to study the energy-saving effect considering both the shading and the power supply gain of a PV roof, a simplified heat transfer calculation model of a PV roof is proposed by analyzing the energy-saving mechanism of the PV roof. The overall energy-saving efficiency index of a PV rooftop is introduced. In addition, 13 typical cities in 5 climatic regions of China are selected for the investigations to evaluate the overall energy-saving performance of three PV roof types. Based on the obtained results, the following conclusions are drawn.

(1) The overall energy-saving efficiency values of 13 typical cities in the summer were in the range of 0.25–0.35. The roof with a horizontal PV had the highest efficiency of 0.32. In the winter, the overall energy-saving efficiency varied from 0.29 to 0.97. In contrast, in the summer, the roof with a tilted PV had the highest efficiency of 0.97. Among the selected regions, in the cold and severely cold regions with a large temperature diurnal range and low average temperature, the energy-saving efficiency was relatively high.

(2) According to the obtained results, a horizontally-mounted PV roof is more suitable for the summer season, and when possible, in hot-summer and warm-winter area, the installed PV module should be removed at night so that the roof can radiate the long-wave radiation to the environment, thereby making the shading benefit positive. Nevertheless, a tilted PV roofs is more suitable for the winter season. Further, the overall energy-saving efficiency is relatively high in the cold and severely cold regions where the daily temperature diurnal is large, and the average temperature is relatively low.

(3) In summary, the proposed simplified calculation method and the presented results on the overall energy-saving efficiency of PV rooftops have large application scope. For the tilted PV roof, this paper took 30° as the inclined angle, but the specific installation and the actual energy-saving effect should be determined after detailed analysis according to the local latitude and other conditions. In addition, if the meteorological conditions in other parts, such as the intensity of solar radiation, temperature, wind speed, and others, are similar or close to those of 13 typical cities in China studied in this work, the conclusions drawn in this paper can also be used as a reference.

Declaration of Competing Interest

The authors declare that they have no known competing financial interests or personal relationships that could have appeared to influence the work reported in this paper.

Acknowledgement

This work was supported by the National Natural Science Foundation of China [Nos. 51590911, 51678468], the National key research and development program [No. 2016YFC0700400], the Shaanxi Youth Science and Technology Nova project [No. 2017KJXX-22] and Cardiff University Global Challenges Research Fund HABITAT project.

Appendix A. Thermophysical parameters of components

Material	**Conductivity λ (W/(m·K))**	**Density ρ (kg/m^3)**	**Specific heat capacity c (kJ/(kg·K))**	**Thickness *d* (m m)**
PV modules:				
glass cover-plate	1.04	2500	0.835	4
upper EVA glue	0.21	938	1.56	0.5
PV battery pack	150	1650	0.7	0.3
lower EVA glue	0.21	938	1.56	0.5
TPT back panel	0.14	1475	1.13	3

Material	Conductivity λ (W/(m·K))	Density ρ (kg/m^3)	Specific heat capacity c (kJ/(kg·K))	Thickness *d* (m m)
Roof structure:				
slag or stone	1.436	881	1.67	12
waterproof layer	0.19	1121	1.67	10
insulating layer	0.043	91	0.841	50
Concrete layer	1.731	2243	0.841	150

Appendix B. Simulation variables

Variable	Description	Data source
e	Wind speed coefficient for h_c (roof surface /PV surface)	6.2/5.62 (Spitler and Nigusse, 2010)
f	Wind speed coefficient forh_c (roof surface /PV surface)	4.3/3.9 (Spitler and Nigusse, 2010)
βr	Roof slope	assumed to be 0°
βp	The inclination angle of the PV module relative to the roof surface	assumed to be30°
αC	Absorptivity of PV battery pack	0.95 (Wang et al., 2006)
εC	Emissivity of PV battery pack	0.84 (Jones and Underwood, 2001)
εb	Emissivity of TPT backsheet	0.893 (National Standard of PR China, 2016)
αr	Absorptivity of the exterior surface of the roof	0.74

Variable	Description	Data source
εr	Emissivity of the exterior surface of the roof	0.9
Ti	Indoor air temperature	18°Cin winter; 26°Cin summer
hi	The heat transfer coefficient of the internal surface of the roof and the indoor air	8.7 W/(m^2·K)
cop	Performance coefficient of air conditioning system	3.72

Appendix C. Details of typical cities

No.	Zone Type	City	Geographical position		Annual radiation MJ/m^2·a	Outdoor air temperature (°C)	
			longitude	latitude		Tmax	Tmin
①	I-severe cold	Golmud	94.89°	36.42°	7010.5	35	−18.6
②	II-severe cold	Xining	101.78°	36.62°	5927.3	30.8	−19.5
③	III-severe cold	Chifeng	118.87°	42.26°	5496.3	35	−25.1
④	IV-severe cold	Harbin	126.53°	45.80°	4764.2	33.6	−30.3
⑤	I-cold	Lhasa	91.17°	29.65°	7218.1	29.5	−11.1
⑥	II-cold	Kashi	75.99°	39.47°	6050.8	37.7	−15.8
⑦	III-cold	Beijing	116.41°	39.9°	5119.8	40.3	−12.5
⑧	IV-cold	Dandong	124.35°	40.00°	4387.6	30.7	−27.1
⑨	IV-hot summer and cold winter	Wuhan	114.31°	30.59°	4217.1	38.7	−2.6
⑩	V-hot summer and cold winter	Chongqing	106.55°	29.56°	3108.2	40.7	1.7
⑪	warm	Kunming	102.83°	24.88°	5416.1	29.7	−1.9

No.	Zone Type	City	Geographical position		Annual radiation MJ/m²·a	Outdoor air temperature (°C)	
			longitude	latitude		Tmax	Tmin
⑫	hot summer and warm winter	Guangzhou	113.26°	23.13°	4087.6	36	4.7
⑬	hot summer and warm winter (high temperature)	Sanya	109.51°	18.25°	6200.3	34.5	13.7

References

Ali et al., 2018, A preliminary feasibility of roof-mounted solar PV systems in the Maldives,. Renew. Sustain. Energy Rev., 83 (3) (2018), pp. 18-32

ASHRAE, 1997 ASHRAE Handbook of Fundamentals (SI Edition), Atlanta, GA, USA (1997)

Bai et al., 2015, Characteristic output of PV systems under partial shading or mismatch conditions, Sol. Energy, 112 (2015), pp. 41-54

Ban-Weiss et al., 2013, Electricity production and cooling energy savings from installation of a building-integrated PV roof on an office building, Energy Build., 56 (1) (2013), pp. 210-220

Bigot et al., 2009, A nodal thermal model for PV systems: impact on building temperature fields and elements of validation for tropical and humid climatic conditions, Energy Build., 41 (1) (2009), pp. 1117-1126

Davis et al., 2001, Prediction of building integrated PV cell temperatures, J. Sol. Energy Eng., 123 (3) (2001), pp. 200-210

Dehwah and Asif, 2019, Assessment of net energy contribution to buildings by rooftop PV systems in hot-humid climates, Renew. Energy, 131 (2) (2019), pp. 1288-1299

Dominguez et al., 2011, Effects of solar PV panels on roof heat transfer, Sol. Energy, 85 (9) (2011), pp. 2244-2255

Duffie et al., 1980, Solar Engineering of Thermal Processes, Wiley (1980)

Ghoddami and Yazdani, 2011, A single-stage three-phase photovoltaic system with enhanced maximum power point tracking capability and increased power rating, IEEE Trans. Power Deliv., 26 (2011), pp. 1017-1029

Jones and Underwood, 2001, UnderwoodThermal model for PV systems, Sol. Energy, 70 (4) (2001), pp. 349-359

Jung, 2014, Optimal Control Methods for PV-integrated Shading Devices, Doctoral dissertation, University of Michigan (2014)

Kapsalis and Karamanis, 2015, On the effect of roof added photovoltaics on building's energy demand, Energy Build., 108 (2015), pp. 195-204

Kapsalis et al., 2014, Simulation of the cooling effect of the roof-added photovoltaic panels, Adv. Build. Energy Res., 8 (1) (2014), pp. 41-54

Kotak et al., 2014, Installation of roof-top solar PV modules and their impact on building cooling load, Build. Serv. Eng. Res. Technol., 35 (6) (2014), pp. 613-633

Mani and Pillai, 2010, Impact of dust on solar photovoltaic (PV) performance: research status, challenges and recommendations, Renew. Sustain. Energy Rev., 14 (9) (2010), pp. 3124-3131

National Standard of PR China, 2016. Thermal Design Code for Civil Building (GB50176-2016). China Planning Press, Beijing (in Chinese).

Oliver and Jackson, 2001, Energy and economic evaluation of building-integrated photovoltaics, Energy, 26 (4) (2001), pp. 431-439

Palyvos, 2008, A survey of wind convection coefficient correlations for building envelope energy systems' modeling, Appl. Therm. Eng., 28 (8–9) (2008), pp. 801-808

Peng and Lin, 2013, Investigation on the development potential of rooftop PV system in Hong Kong and its environmental benefits, Renew. Sustain. Energy Rev., 27 (12) (2013), pp. 149-162

Pérez-Lombard et al., 2008, A review on buildings energy consumption information, Energy Build., 40 (2008), pp. 394-398

Renaudineau et al., 2011, A new approach in tracking maximum power under partially shaded conditions with consideration of converter losses, Sol. Energy, 85 (2011), pp. 2580-2588

Salamanca et al., 2016, Citywide impacts of cool roof and rooftop solar photovoltaic deployment on near-surface air temperature and cooling energy demand, Bound.-Layer Meteorol., 161 (1) (2016), pp. 203-221

Shao et al., 2019, Experimental study on electrical and thermal performance and heat transfer characteristic of PV/T roof in summer, Appl. Therm. Eng., 162 (2019), pp. 114-276

Spitler and Fisher, 1999, On the relationship between the Radiant Time Series and Transfer Function Methods for design cooling load calculations, HVAC&R Res., 5 (2) (1999), pp. 123-136

Spitler and Nigusse, 2010, Refinements and improvements to the radiant time series method, ASHRAE Trans., 116 (1) (2010), pp. 542-549

Topić et al., 2017, The mathematical model for finding an optimal PV system configuration for the given installation area providing a maximal lifetime profit, Sol. Energy, 144 (2017), pp. 750-757

Wang et al., 2006, Influence of a building's integrated-PVs on heating and cooling loads ,Appl. Energy, 83 (9) (2006), pp. 989-1003

Wang et al., 2017, Study on comprehensive energy-saving of shading and photovoltaics of roof added PV module, Energy Procedia, 132 (2017), pp. 598-603

Wiginton et al., 2010, Quantifying rooftop solar photovoltaic potential for regional renewable energy policy , Comput. Environ. Urban Syst., 34 (4) (2010), pp. 345-357